Evaluation of Hygroscopic Cloud Seeding Flares

Roelof T. Bruintjes, Vidal Salazar, Trudi A. Semeniuk[2], Peter Buseck[2],
Daniel W. Breed and Jim Gunkelman[1]
Research Applications Laboratory, National Center for Atmospheric Research, Boulder, Colorado
[1]Ice Crystal Engineering, Davenport, North Dakota
[2]Arizona State University, Tempe, Arizona

ABSTRACT. A test facility has been designed to provide a reproducible environment for combustion of flares and measurement of the resultant particles. The facility provides a simulation of the environment that a flare would encounter from an aircraft. The facility was used to evaluate the concentrations, sizes and chemistry of many flares with different chemical formulations.

Earlier studies of particle sizes produced by the South African flares indicated that a cooler burning flare could potentially produce larger particles. However, initial field studies in 2002 did not support this hypothesis. Small particles were dominant at both the beginning and end of the flare burn, when the burn was coolest,. In addition, comparison of the Ice Crystal Engineering (ICE) 65% and 70% potassium perchlorate-containing flares indicates that the 70% flare produced larger particles, despite having more oxygen present to yield a hotter burn.

The main characteristic of the production of particles by the flare during a burn is that the variations in the total concentration of the particles are small. However, the concentrations of larger particles (>1μm diameter) varies substantially during the individual flare burns and from flare to flare. The latter variations seems to be due to the manufacturing process, including variations in the chemical composition (mesh size, purity, reactions within chemical species, etc) and the cover tube the flare material is compressed in. These changes in the particle size need to be explored further.

Comparisons among the particle spectra from the ICE 65, 70 and 80% $KClO_4$ hygroscopic flares showed that an increase in the amount of the hygroscopic salt ($KClO_4$) seem to slightly increase the number of larger particles. The larger proportion of the oxidizing salt gives a higher burning temperature, shifting the final size distribution towards larger particle sizes. Based on Scanning and Transmission Electron Microscopy (SEM and TEM) analyses of the ICE 70% flare it seems that the larger particles produced by the flares are composed of aggregate mixtures of KCl and $Ca(Cl)_2$ and are not single particles. Aggregation or coagulation of particles is thus the primary mechanism producing larger particles.

Based on parcel modeling studies, the new ICE 70% flare produces substantially more drizzle drops at shorter times than the South African flare. After 1 minute, the new ICE flare initiates drizzle and concentrations of drizzle water reach a maximum, when the South African flare just starts producing drizzle size drops. In addition, the drizzle results in a more effective coalescence process, forming rain. Once drizzle is formed, the transformation to rainwater proceeds faster than with the original South African flares. After approximately 10 minutes, the new ICE flare produces nearly two orders of magnitude more drizzle water than the South African flare.

1. INTRODUCTION

In the past fifteen years, a new approach to hygroscopic seeding has been explored in summertime convective clouds in South Africa as part of the National Precipitation Research Programme (Mather et al., 1997; Terblanche et al., 2000), Mexico (Bruintjes et al., 2003; WMO, 2000; NRC, 2003; Silverman, 2003), and Queensland, Australia (Tessendorf et al., 2012). Since then many other countries have also started using this approach. This approach involves seeding summertime convective clouds below cloud base using pyrotechnic flares that produce small salt particles on the order of 0.5μm diameter in an attempt to broaden the initial cloud droplet spectrum and accelerate the coalescence process. The burning flares provide larger cloud condensation nuclei (CCN) (>0.3 μm diameter) to the growing cloud, influencing the initial condensation process and allowing fewer CCN to activate into cloud droplets (Cooper et al., 1997). The larger artificial CCN inhibit the smaller natural CCN from nucleating, resulting in a broader droplet spectrum at cloud base. These fewer cloud droplets grow to larger sizes and are often able to start growing more efficiently by collision and coalescence with other cloud droplets within 15 minutes as shown in a modeling study by Cooper et al. (1997), initiating the rain process earlier within a typical cumulus cloud lifetime of 30 minutes.

The development of this seeding approach was triggered by radar and microphysical observations of a convective storm growing in the vicinity of a large paper mill, with apparent enhancement of coalescence in these clouds compared with clouds further away from the paper mill (Mather, 1991). Earlier observations by Hindman et al. (1977) and Eagan et al. (1978) also suggested a connection between paper mills and enhanced precipitation due to larger hygroscopic particles being emitted into the atmosphere.

There are significant operational advantages to hygroscopic seeding with pyrotechnic flares compared to large particle salt seeding as practiced in Thailand and other Southeast Asian countries. The amount of salt required is much less compared to large bags of salt, the salt particles are readily produced by flares, and the target area for seeding is an identifiable region at cloud base (updraft region) where the initial droplet spectrum is determined (Cooper et al., 1997).

Mather et al. (1997) reported results from a randomized cloud seeding experiment that was conducted from 1991 to 1996 in summertime convective clouds in the Highveld region of South Africa. The results of this experiment indicated that precipitation from seeded storms was significantly larger than from control (unseeded) storms at the 95% confidence level.

Exploratory analyses indicated that seeded storms rained harder and longer than unseeded storms. Mather et al. (1997) provided microphysical evidence that supported the physical hypothesis. It was remarkable that statistical significance was achieved on such a small sample set of 127 storms (62 seeded and 65 controls), suggesting that the seeding signal was strong and readily detected,

The promising results of the South African experiment led to the start of a new program in Mexico in 1996 using the South African hygroscopic flares. The Mexican program was conducted from 1996 to 1998 and included physical measurements and a randomized seeding experiment. Bruintjes et al. (2003), WMO (2000) and Silverman (2003) provide an overview of the experiments and results. The Mexican results were remarkably similar to the results from the South African experiment. Model calculations of Reisin et al. (1996) and Cooper et al. (1997) support the hypothesis that the formation of precipitation via coalescence is accelerated by the large salt particles produced by hygroscopic flares.

This paper reviews the history of the development and use of hygroscopic flares for seeding clouds to enhance rainfall, and the theory behind it, with special emphasis on the production of drizzle drops. As hypothesized by Cooper et al. (1997) the drizzle-size drops may be carried by the strongest updrafts to cloud top where they may spread and be carried down in the downdrafts and near cloud edges and would then spread throughout the cloud (Blyth et al., 1988 and Stith et al., 1990).

Airborne and laboratory measurements of the different particle size spectra will be presented and the possible impacts on the condensation/coalescence process will be explored.

A recently developed test facility to evaluate the chemical composition, size and concentrations of the particles produced by hygroscopic flares will also be described and a preliminary evaluation of newly developed hygroscopic flares will be presented.

2. CCN CHARACTERISTICS: MODELING STUDIES OF CONDENSATION AND COALESCENCE RELATED TO HYGROSCOPIC FLARE SEEDING

Three important parameters underpin the principle of enhancing the coalescence process via hygroscopic seeding, i.e., chemistry (hygroscopicity), size, and concentration of the CCN produced from the flares or large particle salt seeding. The principle of flare seeding is to produce effective CCN (usually salts such as sodium chloride, potassium chloride, or calcium chloride) particles in larger sizes (large or giant nuclei) than occur in the natural environment. The effectiveness of seeding will also depend on the nature and concentration of natural background particles.

The flares used in the South African and Mexican experiments provided larger CCN (>0.3 μm diameter) to the growing cloud (Hindman et al, 1977). Cooper et al. (1997) showed that if the CCN introduced into the cloud from the flare are larger in size than the natural CCN, then the CCN from seeding will activate preferentially over the natural CCN and change the character of the drop size distribution in favor of coalescence and formation of rain. Thus, the larger artificial CCN inhibit the smaller natural CCN from nucleating, resulting in a broader droplet spectrum at cloud base. These fewer cloud droplets grow to larger sizes, and are often able to start growing by collision and coalescence with other cloud droplets within 15 minutes, initiating the rain process earlier within a typical cumulus cloud lifetime of 30 minutes.

The calculations of Reisin et al. (1996) and Cooper et al. (1997) support the hypothesis that the formation of precipitation via coalescence is accelerated by the salt particles produced by the flares. These studies found that for clouds with a maritime cloud droplet spectrum, hygroscopic seeding with flares has no effect, since coalescence is already very efficient in such clouds. The relatively high concentrations of large natural CCN prevent the seeded particles from dominating the growth. Thus, clouds with background CCN concentrations less than about 350 cm^{-3} at 1% supersaturation, in maritime environments, do not respond favorably to hygroscopic seeding, since the presence of the large natural nuclei produce large drops, preventing the seeded particles from growing.

Results from these calculations should be interpreted with caution, since they oversimplify the real process of precipitation formation. Cooper et al. (1997) allude to some of these shortcomings related to mechanisms that broaden cloud droplet size distributions, sedimentation, and the possible effects on ice phase processes. These models also do not simulate the complex dynamics in convective clouds. The modeling studies of both Reisin et al. (1996) and Cooper et al. (1997) indicate that the role of the background CCN (size and concentrations) is critical to determining the effectiveness of cloud seeding because the seeded nuclei compete with the background aerosols for the available water vapor.

Cooper et al. (1997) showed that the introduction of giant nuclei, larger than 10-μm diameter, lead to an earlier development of raindrops. Yin et al. (2000a; 2000b) found similar results in their modeling studies using a two-dimensional, slab symmetric cloud model. Yin et al. (2000a) corroborated the hypothesis of Mather et al. (1997) that using flares for seeding hygroscopic particles below cloud base could lead to the broadening of the cloud droplet spectra and an earlier formation of raindrops. These studies indicated that the most effective seed particles were those with radii larger than 1μm, and especially those larger than 10μm; and that particles less than 1μm always had a negative effect on rain development. Although these studies indicated that seeding with particles larger than 10μm in radius were the most beneficial for rain enhancement and promoted the formation of drizzle-droplets and raindrops, the drizzle drops formed were rapidly depleted once the few large privileged drops grew to raindrop size. Cooper et al. (1997) found that the rapid depletion of the drizzle size drops limited the production of other raindrops. As a result, rain develops early, but does not last very long and its contribution to the total rain on the ground is limited. It should be emphasized that the Cooper et al. model does not compute the effect of the drop breakup, a process that could possibly enhance the concentration of drizzle size drops. In contrast, introduction of much higher concentrations of 1 μm particles can lead to competition with the natural CCN. Activation of the seeded particles prevents activation of the natural CCN and in appropriate cases, leads to reduction in the total concentration and broadening of the drop size distribution. This results in initiation of an active coalescence process, in some cases leading to high concentrations of drizzle along with the production of rain. Yin et al. (2000a) found that when they repeated the seeding experiments in their model using the same mass for particles in the range 1-10μm and for those larger than 10μm, the concentration of drizzle drops was substantially larger with the seed particles between 1 and 10μm (Yin et al. 2000a).

Caro et al. (2002) used a detailed microphysical parcel model (Flossman et al. 1985; 1987) to confirm most of the results from the previous modeling studies. Their studies indicated that the most rapid formation of precipitation occurred in the model for very large particle radii (> 15μm). However, they also indicated that smaller seeding particles have the advantage of

increasing the concentration of drizzle size drops, increasing the chance of the seeding material staying in the cloud and dispersing the seeding effect to larger parts of the cloud or neighboring clouds. Although seeding with larger particles increased the production of precipitation in the model, it also risked premature precipitation. For seeding to have an optimum effect, with sufficient concentrations of drizzle size drops, they suggested a mean seed particle diameter between 0.5 and 6μm. Segal et al. (2004) found similar results.

Yin et al. (2000a), Caro et al. (2002) and Segal et al. (2004) alluded to the potential effects on ice processes that could possibly enhance precipitation formation. Although the models used in these studies were different, one of the main conclusions that emerged is that the seeded particles have to be larger than 0.5 μm and preferably between 1 and 10μm diameter to produce substantial concentrations of drizzle size drops in a cumulus congestus cloud with updrafts near cloud base ranging from 1 to 4 ms-1.

3. AIRBORNE MEASUREMENTS OF FLARE PARTICLES

The only measurements of the particle spectra produced by the flares in the literature are those presented by Mather et.al. (1997; Fig. 7) from South Africa. These airborne measurements were obtained by flying an aircraft equipped with particle measuring probes about 50 m behind the seeding aircraft. Mather et al. used a Passive Cavity Aerosol Probe (PCASP) to measure the concentration of particles between 0.1 and 3μm in diameter in 15 size bins, a Forward Scattering Spectrometer Probe (FSSP-100) to measure the concentration of particles between 2 and 47μm in diameter in 15 size bins, and a 2-D Optical Array Probe to measure particles between 50 and 1000μm in diameter.

The size distribution measurement of the dry particle sizes by Mather et al. (1997) indicate that a majority of the number of particles produced from the magnesium/potassium perchlorate flares are less than 0.5μm diameter. However, the measurements also indicated that a tail of larger particles was produced extending out to about 10μm diameter. These larger particles are extremely important as pointed out in the modeling studies discussed in the previous section. Most of the modeling studies used the South African spectra; however, these are the only measurement of the particle spectra produced by the burning flares and their reproducibility is unkown.

Another measurement campaign was conducted in Texas in 1997 to assess the particle spectra produced by different flares from different manufacturers as well as the original South African flare. The measurements were conducted in the same manner as the original South African measurements by flying an aircraft equipped with particle measuring probes about 50 to 100 m behind the seeding aircraft. The primary instruments measuring the particle spectra from the burn-in-place 1kg flares were a PCASP and FSSP-300 probe. The FSSP-300 is a modified version of the FSSP-100 probe measuring particles in 31 size bins between 0.3 and 20μm in diameter. In addition, a University of Wyoming CCN counter was flown on theaircraft to assess the CCN activity of the particles produced by the flares. The CCN counter was run at a constant supersaturation of 0.3%.

The purpose of the measurements was to determine the reproducibility of the South African measurements and any differences in particle spectra between flares from different manufacturers. The particle spectra of four different types of flares were measured: the original South Africa flare, a flare manufactured by Atmospherics Incorporated, a French flare, and a modified version of the original South African

flare called D383 (containing less Mg, 2.5% versus 5.0% in the original South African flare and replacing the NaCl in the original flare with $CaCl_2$).

Figure 1 displays the combined size spectra measured by the PCASP and FSSP-300 aerosol probes for the four different flares (D383 – Modified South African flare **(**a), SA – original South African flare (b), AI - Atmospheric Incorporated flare (c), and French flare (d)). The measurements were obtained by flying the research aircraft behind the seeding aircraft while the flares were burning. The spectra were averaged over a ten second period. Differences between the spectra from the PCASP and FSSP-300 probes, especially for size ranges larger than 0.3μm diameter, could be due to deliquescence of hygroscopic flare particles at the ambient relative humidities encountered during the flight (between 50 and 70%). The PCASP de-icing heaters tend to dry the aerosols, thus measuring dry particle size, whereas the FSSP-300 measures their wet diameter. Strapp et al. (1992) in a study comparing measurements from the PCASP and FSSP-300 probe found similar results.

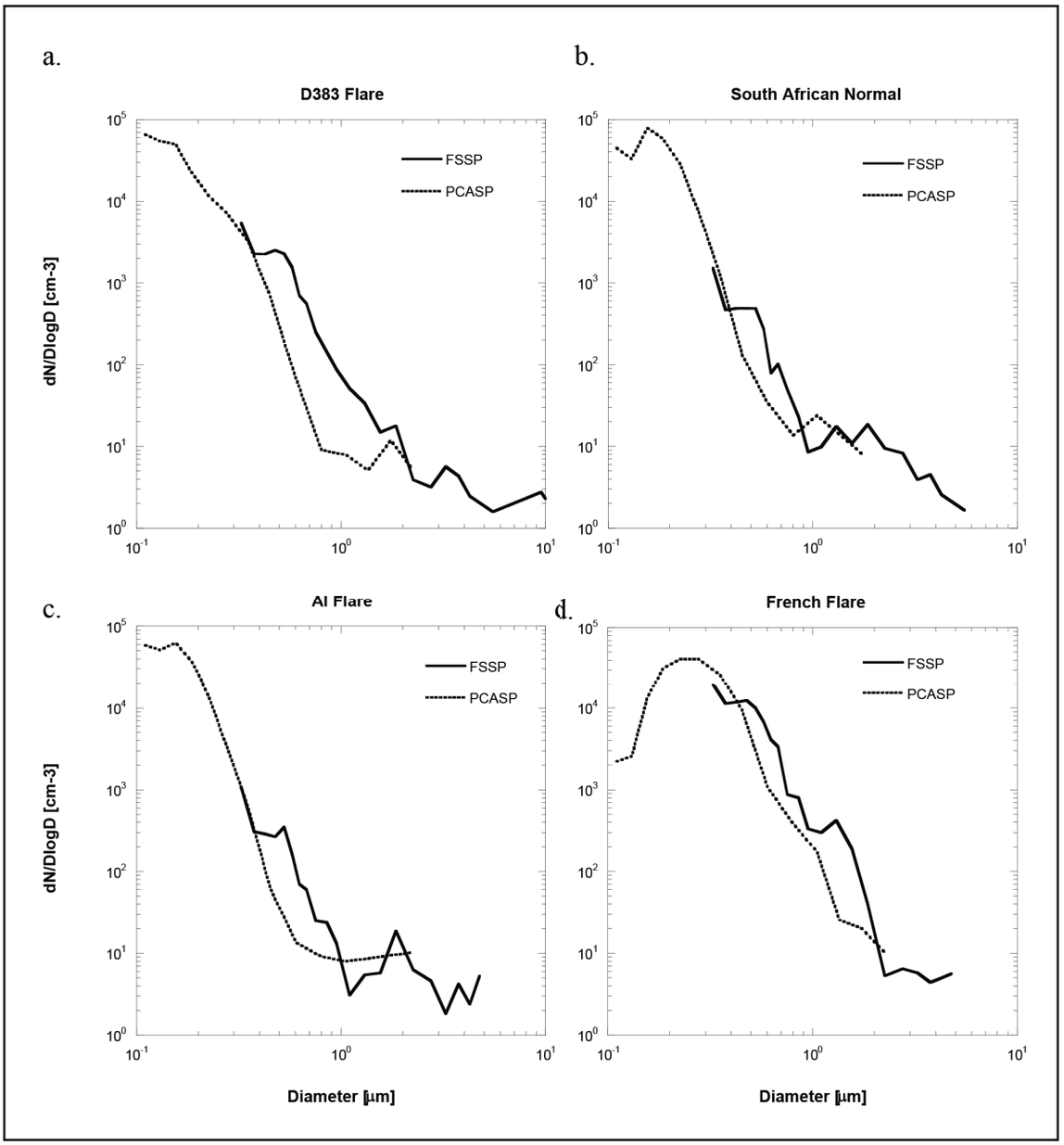

Figure 1. Combined dry aerosol size spectra from four different hygroscopic flares as measured by PCASP and FSSP-300 probes.

There are substantial differences among particle spectra produced by the different flares. The French flare produced the largest mean size, while the AI flare had the smallest mean sizes. Both the original South African and D383 flares produced more particles within the 0.3 to 1μm size range than the AI flare, but less than the French flare. Peak concentrations for the AI flare were around 0.2μm, the South African and D383 flares around 0.3μm and the French flare around 0.4 to 0.5μm. The CCN measurements indicated that all the flares produced particles that are highly active as CCN, resulting in concentrations of more than 2000 cm-3 for all flares.

All four flares showed a tail in the particle spectra extending out to several microns, with the D383 flare producing particles up to 10 μm diameter. Observed concentrations of large particles were highly variable during the burning of the flare, in part due to low concentrations and limited sampling volume. Hence, real concentrations in this size range are difficult to estimate accurately. Significantly, there were remarkable differences in the spectra obtained in Texas from the original South African flare compared with the Mather et al. (1997) measurements. Since modeling studies have highlighted the tail of the spectra as the most important size range for initiation and evolution of coalescence in a cloud, the differences in the South African flare spectra will be further addressed below.

It should be emphasized that it is difficult to obtain measurements of the particle sizes produced by burning flares in flight. It requires two aircraft, one to generate the seeding material, and another to make the measurements. Environmental changes in humidity, temperature, and speed changes of the seeding aircraft, all possibly impact the particle size distribution produced by the flares. In addition, the small size of the plume presentsproblems for sampling especially in a turbulent environment. However, airborne measurements are important as in situ evidence for particle behavior in the atmosphere.

4. FLARE COMPOSTION AND THE EFFECTS ON PARTICLE SPECTRA

Modeling suggested that most effective seeding for the formation of enhanced concentrations of drizzle drops occurs when the introduced CCN have a size of approximately 1μm or larger and the optimum seed particle sizes are between 1 and 6μm in diameter. In our study, we investigated flare composition to determine whether larger particles can be produced that more closely fit the parameters important for drizzle formation. In addition, the model studies suggested that the use of calcium salts in the seeding material could enhance the effectiveness and calcium salts were also included in the tests.

Most hygroscopic flares currently in use are based on the formula of Hindman (1978) developed to initiate fog for cover of military vessels. They are composed of potassium perchlorate, magnesium powder, and a hydrocarbon binder as the oxidizer and fuel respectively. They also incorporate sodium or calcium chloride and lithium carbonate. The products of combustion are a mixture of magnesium oxide, potassium and sodium chlorides, and lithium oxide. In laboratory analyses of South Africa flares, it was found that the flares consisted of a mixture of potassium perchlorate ($KClO_4$), sodium chloride (NaCl), Lithium Carbonate (Li_2CO_3), Magnesium (Mg) and a hydrocarbon binder. Mg powder provided the heat, while $KClO_4$ provided the oxygen for combustion. Stoichiometric analysis indicates that 72% of the oxygen for combustion was provided by the $KClO_4$ and the remainder from atmospheric oxygen.The laboratory particle analyses using scanning electron microscopy indicated that the particles produced in the combustion process closely represented the initial composition of the flares. Data for small and large (>10μm) particles indicated that the small particles constituted most of the mass.

Based on the TEM analysis, Table 1 shows that large particles have a slight enrichment in Mg and a reduction in KCl. In general, the mole fractions of chemical components present in the flare and individual particles were similar. Analyses were not able to detect Li_2CO_3 in the initial flare material or in the particles produced when burned. The reason for this is not known.

TABLE 1. Chemical composition of the original South African Flare and the relative chemical compositions of small (<10μm) and large particles >(10μm) from SEM data.

Chemical Components	Flare Composition	Small Particles	Large Particles
KCL ($KClO_4$)	0.54	0.58	0.42
Na Cl	0.20	0.23	0.25
MgO (Mg)	0.24	0.19	0.33
Li_2CO_3	0.03	Not detected	Not detected

Examination of SEM micrographs of seeding particles captured on glass slides suggest that the salt particles produced in the burning of flares nucleate on MgO (Kok and Mather, unpublished data, 1995). The combustion temperature of the flares is unknown, but is most likely in excess of 2000C (attempts were made to measure the temperature but elements that measured up to 2000C were all burned). Both NaCl and KCl melt at around 800C, and sublime or boil at about 1500C. Under these combustion conditions, the salts will volatilize and then re-condense rapidly, forming small particles. It was hypothesized that if the burning temperature of the flare could be reduced, there would be less volatilization, and consequently formation of larger particles. To test this theory, the South African D383 flare (discussed in the previous section) was manufactured. It contains less Mg (2.5% versus 5.0%) than the original South African flare) and uses $Ca(Cl)_2$ instead of NaCl . Although the D383 flare had higher concentrations of particles in the 0.5 to 1μm range, and had the largest particles present (Figure 1), the overall concentrations were not significantly different from the original South African flare. A flare that uses calcium salts and decomposition of an azorcarbamide compound has also been tested. The “fuel” in this flare is typically used in pyrotechnics, and burns at less than 100C. Several new flare formulations were developed by ICE in North Dakota in our attempt to increase particle sizes. These flare formulations use different salts (sodium chloride, potassium chloride or calcium chloride) and different types of organic binders.

5. FLARE TEST FACILITY

A test facility was designed and constructed to simulate the burning of flares on the wing of an aircraft to address the limitations of aircraft measurements of flare particle spectra and the need for a systematic study on the particles generated by airborne hygroscopic cloud seeding flares. This test facility provides a reproducible environment for the combustion of flares and the measurement of the resultant particles. The facility was used to examine the different commercially produced seeding flares as well as the new formulations described above. A schematic diagram of the test facility is shown in Figure 2.

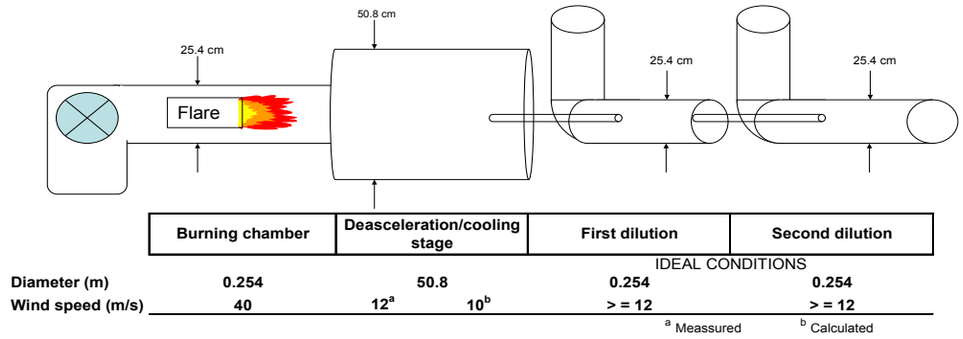

Figure 2. Schematic design of the flare test facility.

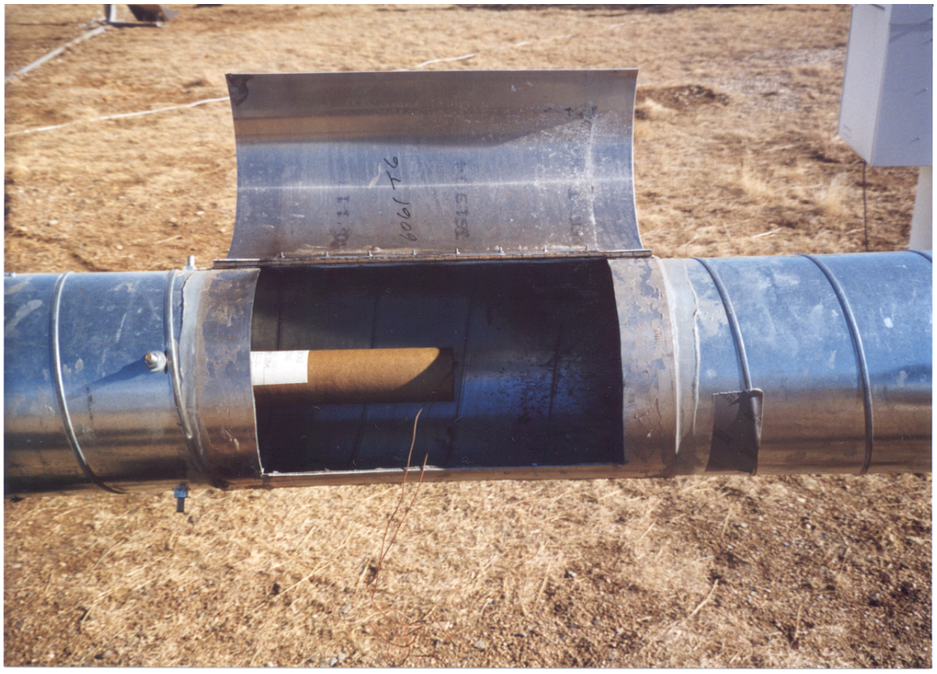

Figure 3. Photograph of the combustion section of the test facility with a flare mounted.

Flares are mounted near the head of the combustion section, aligned axially with the airflow (Figure 3). The burning end of the flare is on the downstream side. This simulates burning a flare on a rack mounted on an aircraft wing. The airflow is sufficient to disperse and cool particles as they are produced. During operation, the combustion section is closed, and the flare is ignited using an electrical igniter.

One of our main considerations when designing the flare testing facility was to ensure continuous sampling of the flare material, without enhancing the collection of eitherenhancing the collection of either small or large particles. Isokinetic sampling was the ideal method for obtaining size distributions of the particles produced by the flare. Figure 4 shows different sampling scenarios (sub-isokinetic, isokinetic and super-isokinetic) with their gravitational losses for different inlet sizes. In a sub-isokinetical sampling (Figure 4a) the gravitational losses of larger particles are enhanced. During a super-isokinetic sampling (Figure 4b) the gravitational losses of smaller particles are enhanced, During a super-isokinetic sampling (Figure 4b) the gravitational losses of smaller particles are enhanced, generating higher concentrations of larger particles and decreasing total particle concentrations. Preferential sampling of larger or smaller particles is evident as the sampling tube diameter becomes smaller. The test facility uses a sampling tube of 1 cm in diameter and 1m in length for both inlets in the dilution stages. This results in an isokinetic sampling procedure that gives a gravitational loss of less than 80% for particles smaller than 10µm diameter. Because we are mainly interested in the large particle tail of the size distribution we focused our analysis on the larger particles.

a)

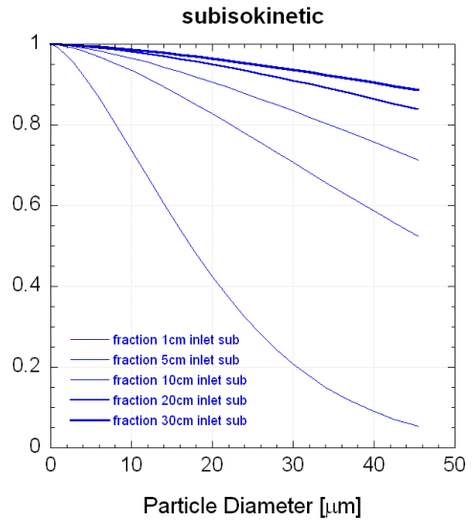

b)

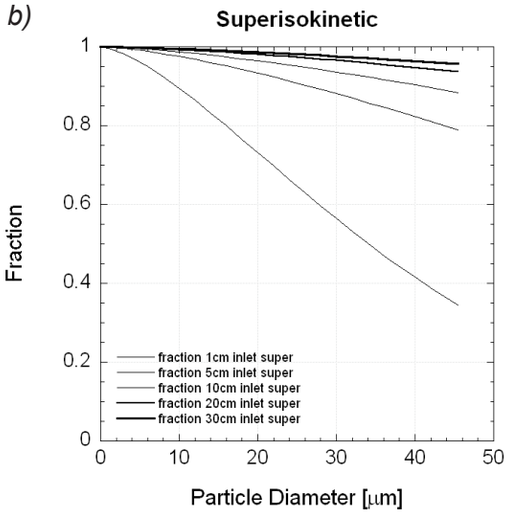

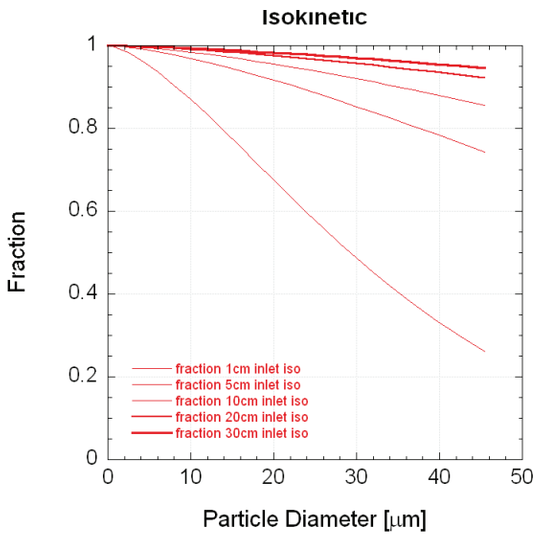

Figure 4. Gravitational losses in a 1 meter long inlet for a sample flow U_o and at a wind speed U = 40m/s and different particle size. a) $U>U_o$, b)$U<U_o$, c) $U=U_o$

Figure 5 shows the characteristics of the completed flare facility, including the calculated and measured wind speeds that minimize gravitational losses and favor isokinetic sampling. A 156,000 lpm (liters per minute) blower is used to provide an airflow of 40 m s^{-1} (no differences were found by varying speeds from 30 to 60ms^{-1}) through the combustion section (stage 1), which is made of circular tubing of 25.4 cm in diameter and 1.5 meters long. The particles in stage 2 (Figure 5) are then collected by a circular copper tubing (stage 3), 1 cm in diameter and 1 meter long, and transported to the first dilution stage (stage 4). The first dilution is fed with clean air at a rate of 12 m/s to match the incoming wind speed ($U=U_o$) in order to sample the particles isokinetically. To dilute the particles further, to satisfy the counting limitations of the particle counters, a second stage dilution (stages 5 and 6) was implemented. The second stage dilution procedure is identical to the first, with a wind blower of 12 m/s to maintain a steady flow of particles to the measuring instruments.

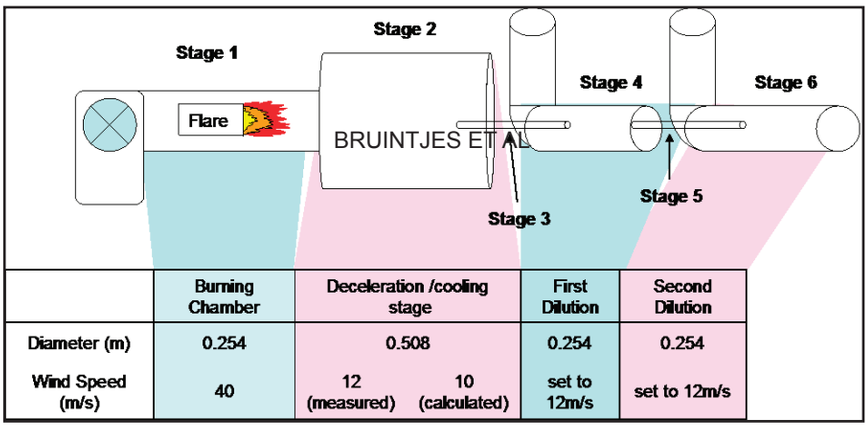

	Burning Chamber	Deceleration /cooling stage		First Dilution	Second Dilution
Diameter (m)	0.254	0.508		0.254	0.254
Wind Speed (m/s)	40	12 (measured)	10 (calculated)	set to 12m/s	set to 12m/s

Figure 5. Dynamic characteristics and an actual photo of the flare facility design.

The diluted smoke is sampled by an array of instrumentation: 1) a CCN counter which measures particles from approximately 0.01-1.0μm diameter and 2) a PCASP which optically sizes and counts particles from 0.1 to 3.0 μm diameter, and 3) a FSPP which measures particles from approximately 3-8μm diameter. All of the data from these particle counters are recorded on a laptop computer. Auxiliary measurement of ambient temperature and relative humidity are also made at the site. Experiments carried out when the relative humidity is 40% or less to be able to compare dry particle sizes. At this relative humidity, particles may hydrate, but they will not grow in size. Ambient temperatures varied between 10 to 30C, but did not affect particle generation at combustion temperatures of >1500C.

6. FLARE TEST RESULTS

A variety of flare formulations were tested on a number of days. Here, we highlight the capabilities of the test facility and some of the differences observed between the different flare types. The initial tests had two major objectives; 1) to determine the reproducibility of particle spectra from the burning flares by burning several flares of the same type, and 2) to evaluate the particle spectra from newly developed and manufactured flares. More than 20 different flare compositions were evaluated at the test facility.

In addition, there were two important objectives in the evaluation of different flare compositions: to determine concentrations and sizes of the particles produced by the flares as a function of time; and to determine variations in different particle size. Many of the different compositions produced similar or smaller particle spectra to that obtained from the original South African flare, hence we will focus on flares that produced larger particles.

6.1 Particle concentrations and size distributions

Figure 6 a to d shows time series of particle concentrations for different threshold sizes for different flares measured in the test facility. Figure 6a displays the particles produced by flares with magnesium/aluminum alloy in place of the magnesium powder. Figure 6b and c display the particle concentrations and sizes of two flares manufactured by ICE with a similar composition to the South African flare, but with calcium chloride in place of sodium chloride. These flares have 65% and 70% potassium perchlorate, respectively. Figure 6d shows the particles produced by the “standard” South African (SA) flare. The SA flare also uses 65% potassium perchlorate as the oxidizer. The data provide number concentrations of the particles as a function of time in the size ranges 0.2μm and smaller, 0.2-0.4μm, 0.4-0.8μm, and greater than 0.8μm diameter. These size ranges delineate the important particle size regimes highlighted by the modeling studies. The utility and advantages of the flare test facility are clear from Figure 6, since complete time series of the particle spectra produced on flare combustion cannot be obtained from aircraft measurements.

Although total concentrations for the different flares are comparable and show very little variation, large variations as a function of time occur for particle sizes between 0.2 and 0.8μm diameter, with largest variations observed for the two flares manufactured by ICE.

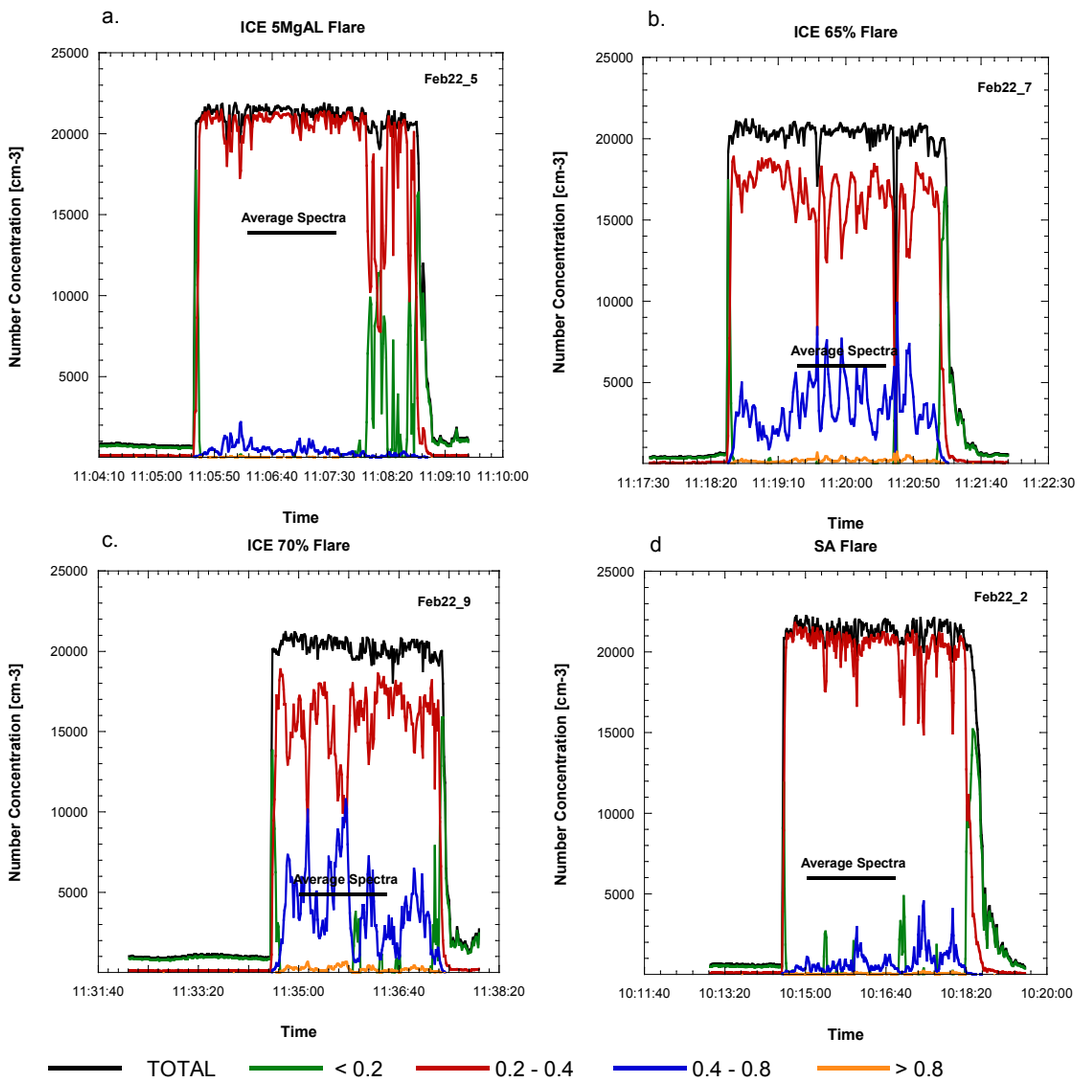

Figure 6. Time history of particle concentrations during flare burns with different compositions.

6.1 Particle concentrations and size distributions

Figure 6 a to d shows time series of particle concentrations for different threshold sizes for different flares measured in the test facility. Figure 6a displays the particles produced by flares with magnesium/aluminum alloy in place of the magnesium powder. Figure 6b and c display the particle concentrations and sizes of two flares manufactured by ICE with a similar composition to the South African flare, but with calcium chloride in place of sodium chloride. These flares have 65% and 70% potassium perchlorate, respectively. Figure 6d shows the particles produced by the "standard" South African (SA) flare. The SA flare also uses 65% potassium perchlorate as the oxidizer. The data provide number concentrations of the particles as a function of time in the size ranges 0.2μm and smaller, 0.2-0.4μm, 0.4-0.8μm, and greater than 0.8μm diameter. These size ranges delineate the important particle size regimes highlighted by the modeling studies. The utility and advantages of the flare test facility are clear from Figure 6, since complete time series of the particle spectra produced on flare combustion cannot be obtained from aircraft measurements.

Although total concentrations for the different flares are comparable and show very little variation, large variations as a function of time occur for particle sizes between 0.2 and 0.8μm diameter, with largest variations observed for the two flares manufactured by ICE.

ICE flares produced significant larger concentrations of particles in the size range 0.4 to 0.8μm diameter than the SA flare (Figs. 6b, c and d). The majority of the particles produced by the SA flare are < 0.3μm diameter. Since the compositions are nominally comparable, differences in the grades of chemicals used, and in the manufacturing procedures must give rise to the differences.

Differences in the amount of potassium perchlorate used in the 65% and 70% ICE flares resulted in larger variations and at times higher concentrations of particles larger than 0.4μm diameter.

Figure 6a shows that modifying the metal fuel used in the flares from magnesium power to a magnesium/aluminum alloy resulted in very small particles. The reason for this change in particle size is not known, but is not beneficial for seeding.

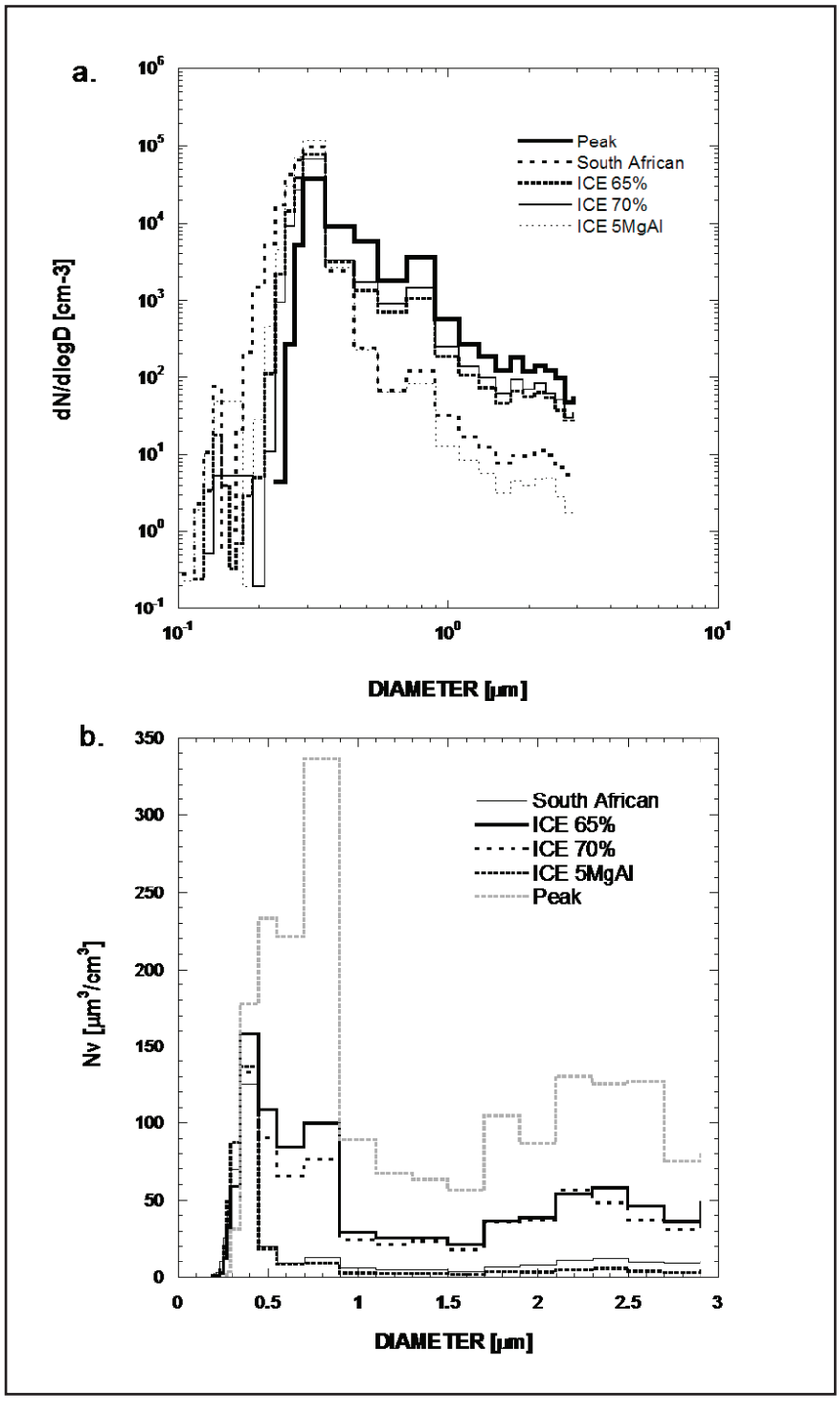

Figure 7. Number size and volume size distributions of flare particles in flares with different compositions

Figures 7a and b display the PCASP number concentration and volume distribution as a function of diameter. The spectra were averaged over the period represented by the horizontal bars in Figure 6. Again, total concentrations are very similar, but ICE 65% and 70% flares have substantially larger concentrations of particles in the size range 0.5 to 3μm diameter. Figure 7b highlights the volume, and hence the mass, of material that is actually produced by the flare. For the ICE 65% flare (Fig. 7b), the maximum number of particles peaks at around 0.3μm, similar to the SA flare, but there is a tail of larger particles that gives a substantial amount of material in the size range larger than 0.5μm. The volume plots for ICE 70% flare show somewhat more mass in the larger particle sizes.

Earlier studies of the SA flares suggested that a cooler burning flare would produce larger particles. However, the data gathered from our studies do not support this hypothesis. In fact small particles dominate the beginning and end of the flare burn when the burn is coolest and comparison between ICE 65% and 70% potassium perchlorate flares showed that the hotter ICE 70% produced larger particles. It appears that concentrations in the size ranges 0.2to 0.4μm and 0.4 to 0.8μm diameter are anti-correlated for the ICE flares, i.e., as particle concentrations in the size range 0.4 to 0.8μm increase, the concentrations in the size range 0.2 to 0.4μm decrease (Fig. 6b and c).

Variations in concentrations of larger particle sizes during the burn occurs for both airborne and ground-based tests and is related to the fact that the flare tube does not burn consistently with time. Burning of flare material can occur inside the tube, or when a section of the tube falls off, in the ambient air, resulting in erratic changes in temperature during the burn In general, larger particles are produced when the burn occurs inside the tube at higher temperatures, and smaller particles when the burning occurs in open air at cooler temperatures. This is consistent with the idea that higher burn temperatures produce larger particles, while cooler burn temperatures produce smaller particles. Different types of tubing could potentially stabilize the burn but these experiments fell outside the scope of the experiments described in the paper.

Ideally, information on the combustion temperatures of different flares is needed; however. Measuring burn temperature directly is very difficult and would require a very expensive optical pyrometer. To obtain relative information on the combustion temperatures of the flares, two platinum resistance temperature probes were mounted within the combustion section. The first probe measured temperature at the tip of the flare, the second measured temperature near the end of the combustion section. We were able to obtain a relative measure of the amount of heat generated during combustion from this temperature differential. Measurements indicated that combustion temperatures of the flares are in excess of 1500C.

Additional formulations were manufactured to study the effects of hotter burning flares on the particle size distribution. In addition, TEM samples were collected to study the chemical composition of different size particles produced by the flares. These tests were carried out on 23 June, 2004 at low relative humidities to measure the dry particle sizes (Fig. 8). Figure 9a shows the time history of the size concentrations of the combusted flare particles (ICE 65%), while Figure 9b displays the associated particle size spectra measured by the PCASP and SPP particle probes. Particle size spectra and burning characteristics were similar to previous flare tests and showed good reproducibility.

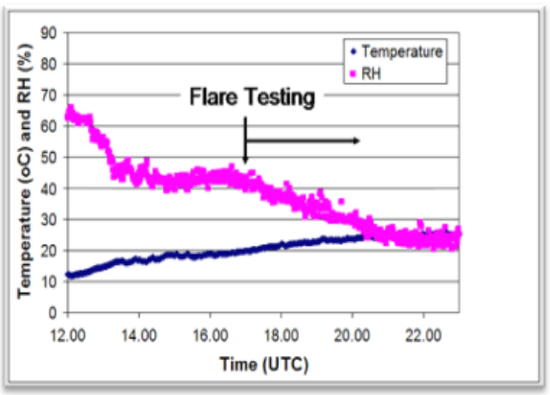

Figure 8. Temperature and relative humidity profile during flare testing on 23 June, 2004.

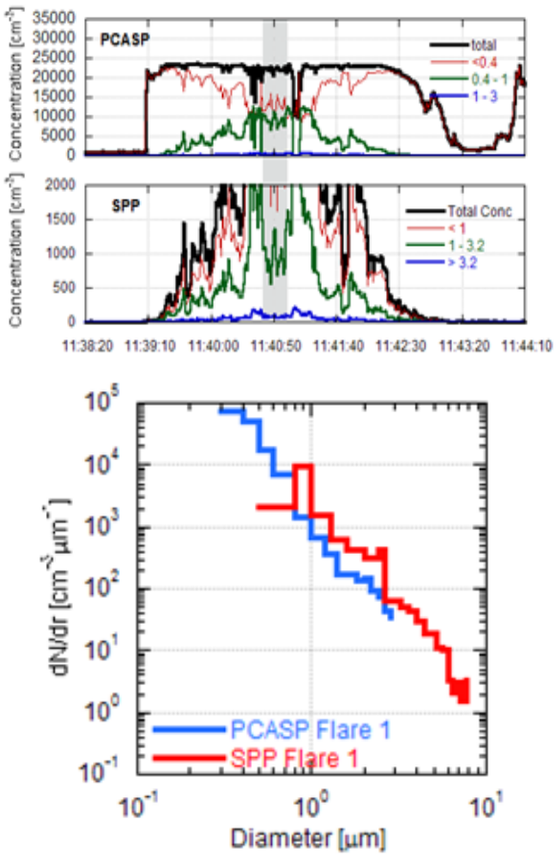

Figure 9. Time history of particle size distributions for combusted flares (a) associated particle size spectra measured by the PCASP and SPP particle probes (b) detailed size spectra for the shaded area in (a) on June 23, 2004.

To investigate the effect of $KClO_4$ on combustion temperature and particle size, flares with 65, 70 and 80% $KClO_4$.were tested. Figure 10 shows the number size distribution for these tests. These size distributions show that an increase in the amount of KClO4 slightly increased the number of larger particles. The ICE 80% flare closely reassembles its predecessor ICE 70%, with only a slight decrease in particle production measured by the PCASP probe and a small increase in concentration of larger particles measured by the FSPP probe. Thus, hotter burning temperature of the ICE 80% shifted the final size distribution towards larger sizes, but only by a small amount. The ICE 70% flare is now the most widely used hygroscopic flare in weather modification programs around the world.

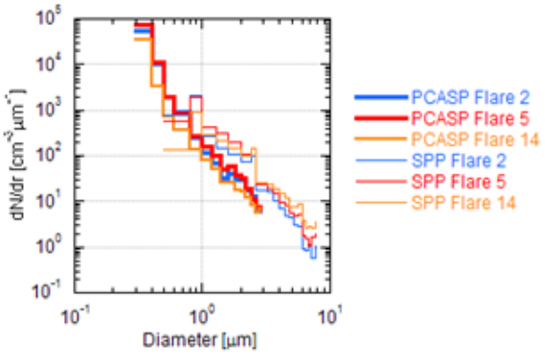

Figure 10. Particle size distributions from flares #2 (ICE 65%), #5 (ICE 70%) and #14 (ICE 80%).

6.2 Chemical composition of combusted particles produced by the ICE 70% flare

An important component of the flare test study was the investigation of the chemical composition of combusted particles, produced by the ICE flares. Individual particles were analyzed using transmission electron microscopy (TEM) at the John M. Cowley Center for High Resolution Electron Microscopy, Center for Solid State Science, Arizona State University.

This method has the unique advantage of providing size, shape, composition, crystallographic structure and speciation information for phase identification and determination to the extent of aggregation. Precise species characterizations can be determined for individual particles as small as 30 nanometers in diameter.

High-resolution imaging (HRTEM) was used to obtain details of features as small as a fraction of a nanometer, remnants of incomplete reactions, and surface coatings. Compositions were determined using energy-dispersive X-ray spectrometry (EDS) for elements heavier than Be.

Samples were collected on carbon-coated TEM grids during the flare tests on 23 June 2004 for the ICE 70% flare burns. Images from these samples show that particles are mixtures of single salt crystals (mostly KCl) and mixed salt aggregates (KCl and $CaCl_2$; Figure 11, 12). Single KCl crystals are typically euhedral and around 0.1μm diameter in size. Mixed salt aggregates are anhedral and typically between 0.8 and 1.5μm diameter. Thus, TEM data show that the larger particles produced by the flares are composed of mixed salt aggregates and are not single particles. Aggregation or coagulation of particles appears to be the primary mechanism producing larger particles.

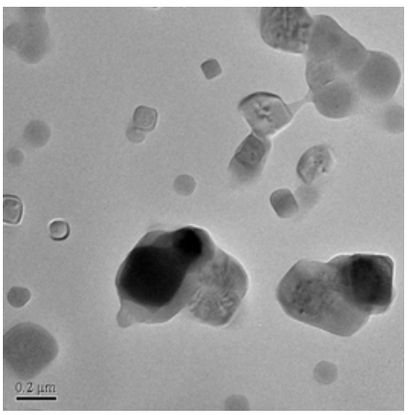

Figure 11. Bright-field TEM image of particles produced by the ICE 70% flare on a film carbon TEM grid.

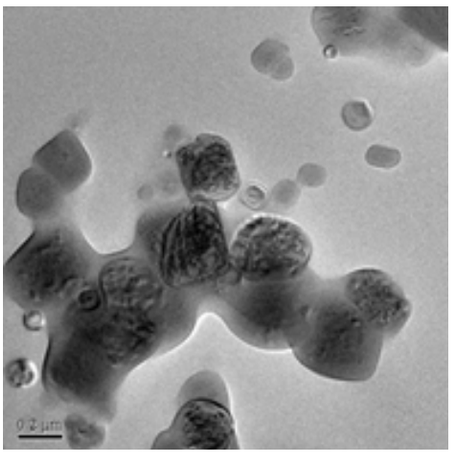

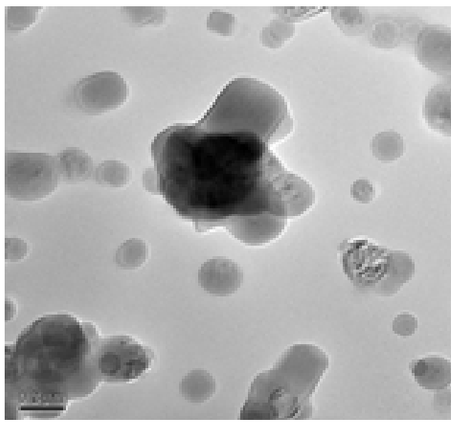

Figure 12. Bright-field TEM images of a) mixed salt aggregates (1.5μm) and smaller CaCl2 particles, and b) mixed salt aggregates (0.2-0.8μm diameter) and smaller CaCl2 particles produced by the ICE 70% flare.

EDS measurements on selected aggregate particles are shown in Figures 13 and 14. The analyses clearly show that cubic particles (~0.6μm diameter) are KCl and coatings are $Ca(Cl)_2$ (Figure 13), suggesting that $Ca(Cl)_2$ enhances aggregation because it remains longer in the liquid stage than KCl. No aggregates of solely KCl were observed.

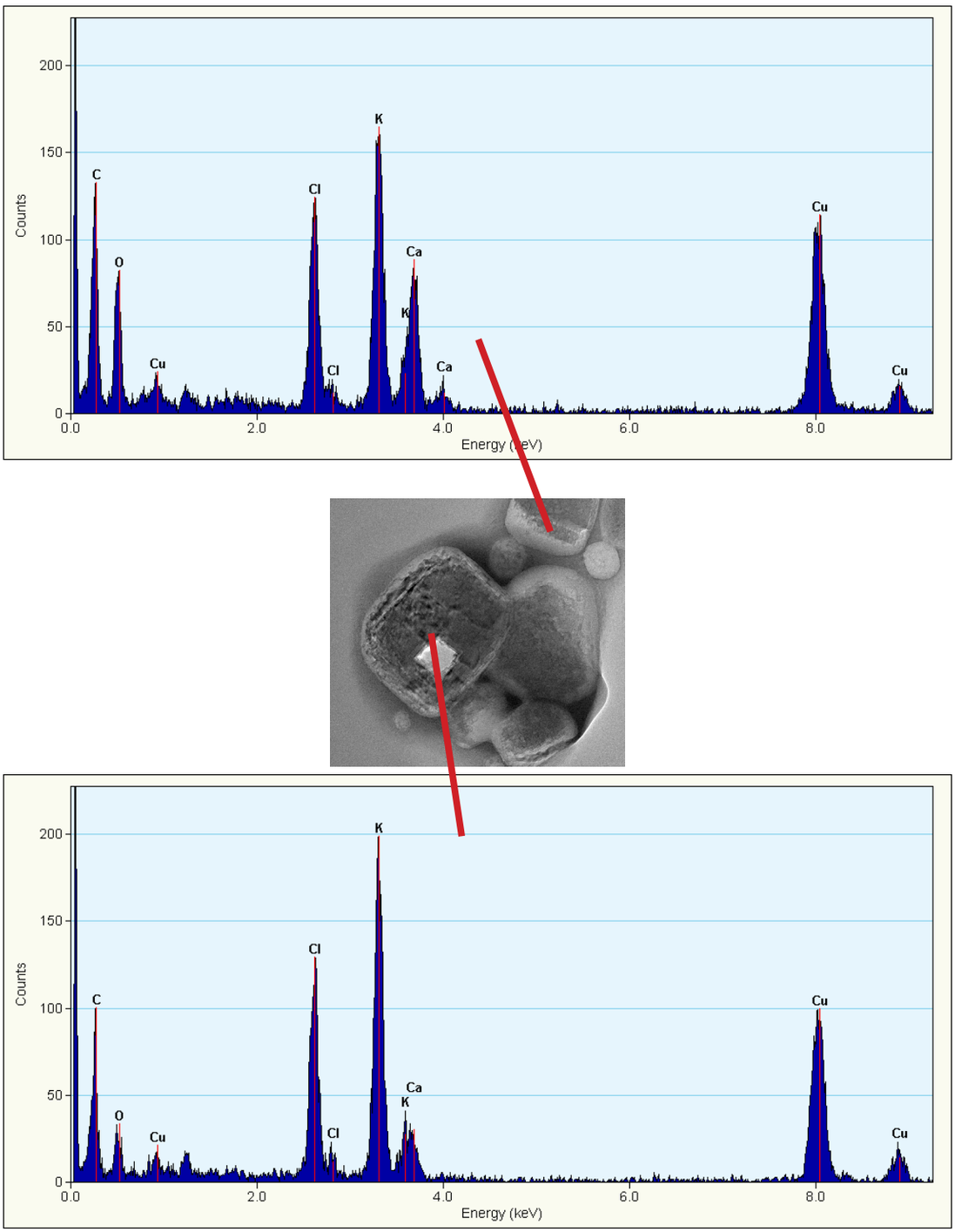

Figure 13. Bright-field TEM image and associated EDS analyses of a mixed salt aggregate (KCl and $CaCl_2$) produced by the ICE 70% flare. Arrows show the locations of EDS measurements. Cu and C are background peaks related to the sample substrate.

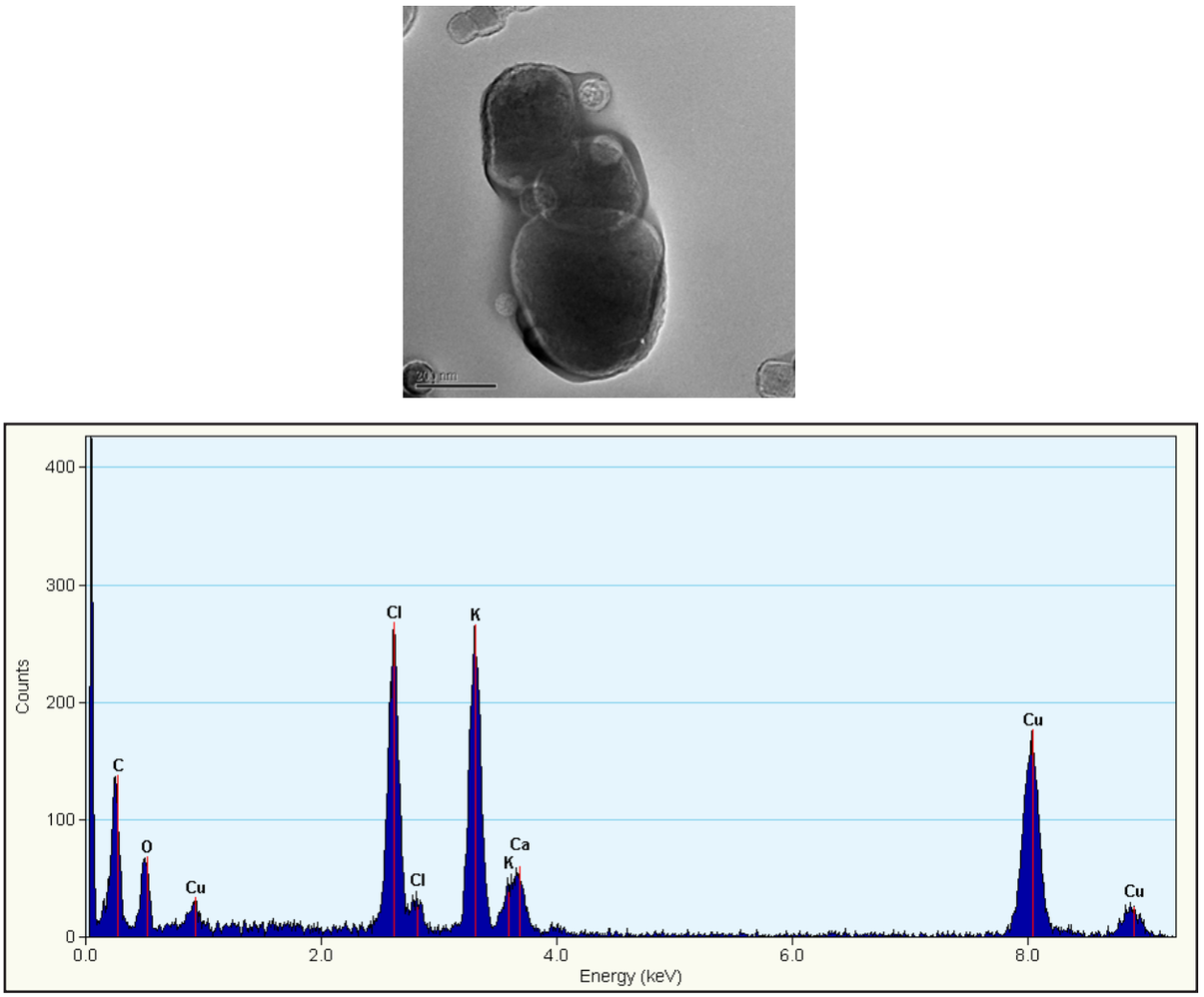

Figure 14. Bright-field TEM image and associated EDS analyses of a mixed salt aggregate (KCl and $CaCl_2$) produced by the ICE 70% flare. Cu and C are background peaks related to the sample substrate.

7. PARCEL MODEL CALCULATIONS TO DETERMINE EFFECTS ON DRIZZLE FORMATION

Combustion particles in the size range 1.0 to 6μm in diameter are substantially enhanced in ICE flares compared with previous flares, including the original South African flare based on the Hindman (1978) formula. We replicated the Cooper et al. (1997) parcel modelsimulations to investigate whether the ICE flare enhances drizzle production compared with the original South African flare, since this flare was specifically developed to increase drizzle concentrations.

The model represents the effects of condensation and coalescence during the adiabatic ascent of a parcel of air. Log-normal curves for particle size distributions from Cooper et al. 1997 and our test facility are displayed in Figure 15. The results of the model calculations are displayed in Figures 16 and 17. The model runs were conducted to show seeding effects,

using the same run characteristics as Cooper et al. (1997). It is clear in Figure 17 that the new ICE 70% flare produces substantially more drizzle mass at shorter times than the South African flare. After 1 minute the new ICE flare initiates drizzle, concentrations of drizzle water reach a maximum at 10 minutes when the South African flare starts producing the first drizzle size drops. The drizzle results in a more effective coalescence process, forming rain faster than for the original South African flare. After approximately 10 minutes, the new ICE flare produces nearly two orders of magnitude more drizzle water than the South African flare. It is important to emphasize that the parcel model studies only indicate the initial response to seeding and after ten minutes the microphysics and dynamics interact and dominate the effects of seeding (Mather et al., 1997; Cooper et al., 1997).

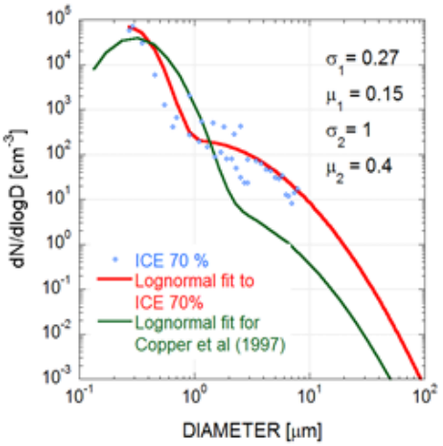

Figure 15. Size distribution of particles published by Copper et al 1997 for the original South African flare (green line) and as measured by our new flare test facility for the ICE 70% flare (red line). The blue dots represent the particle size distribution measured for the ICE 70% at the flare test facility. The characteristics of the 2 lognormal distributions for the ICE 70% flare are shown as an insert.

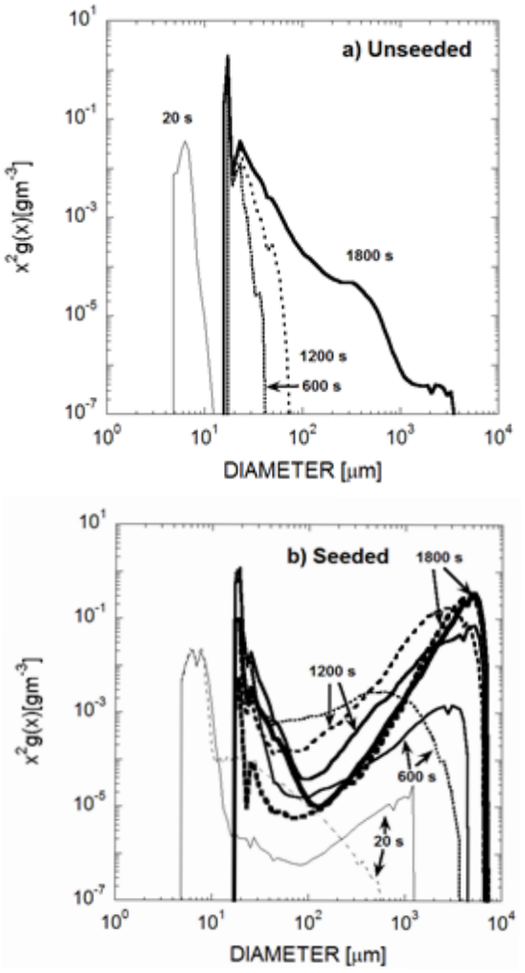

Figure 16. a) Mass distribution functions from Copper et al. (1997) for 20, 600, 1200 and 1800 seconds after passage through cloud base for the unseeded case. b) Mass distribution functions for the seeded case from Cooper et al. (1997) (solid line) and the ICE 70% (dotted line)

These results indicate that the ICE 70% flare is more effective in producing larger drizzle concentrations than the South African flare.

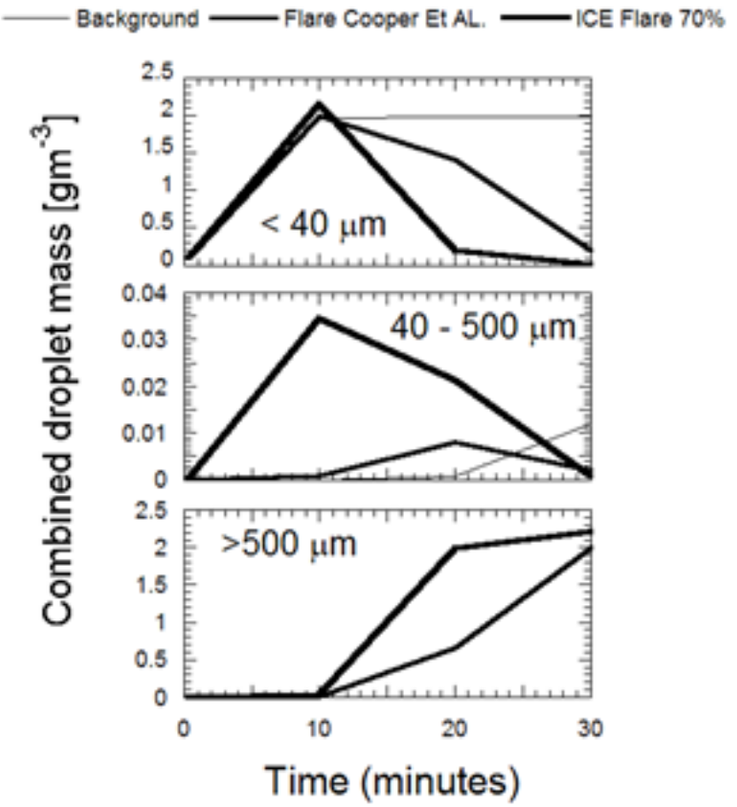

Figure 17. Changes in the distribution of the condensate between cloud droplets (<40μm), drizzle droplets (40 – 500μm) and rain drops (>500μm) after droplet activation: background case (thin solid line), Cooper et al (1997) (medium solid line), and the ICE 70% (thick solid line).

8. DISCUSSION AND CONCLUSIONS

The test facility was designed to provide a reproducible environment for combustion of flares and measurement of the resultant particles. The facility was used to evaluate the concentrations, sizes, and chemistry of flares with different chemical formulations Samples were collected isokinetically such that the characteristics of particle mass, number and size distributions remained unchanged between the different dilution stages. Diffusional and gravitational loss of particles was minimized through careful design of the facility.

In general, we found that variations in the total concentration of the particles produced by flares was small. However, the concentrations of larger particles (>1μm diameter) varied substantially during individual flare burns and among different flare types. These variations reflect both chemical composition (mesh size, purity, reactions within chemical species, flare material, cover material, etc) and manufacturing process.

Our first set of experiments evaluated formulations with cooler burn temperatures, since we surmised that there should be less

volatilization, and consequently the possible formation of larger particles at lower temperatures. Although the new flare formulation (less Mg) had higher concentrations of particles in the 0.5 to 1µm range and the largest particles, the concentrations were not significantly different from the original South African flare. Our second set of experiments evaluated ICE 65, 70 and 80% $KClO_4$ hygroscopic flares. Contrary to earlier aircraft studies of flare material, our test data indicated that larger particles were produced by hotter burn temperatures.

The ICE 70% and 80% flares produced the highest concentrations of particles in size ranges important for drizzle formation.

The conclusion that hotter burning flares produce larger particles is somewhat supported by analyses of natural particles from flaming fires that produce numerous KCl particles (Li et al., 2002; Posfai et al., 2002). The size of the re-condensed KCl particles is likely related to cooling rate. Samples from biomass burning experiments indicate that KCl particles transform to potassium sulfate and potassium nitrate particles within 30 minutes of exposure to atmospheric sulfates and nitrates and these partciles are usually smaller than the original KCl particles and thus less effective in producing large cloud droplets. (Li et al., 2002; Posfai et al., 2002). These rapid transformations have implications for hygroscopic seeding. For example, if hygroscopic particles are not released at cloud base, where they can be directly incorporated into cloud droplets; then chemical reactions could take place that change their chemical and hygroscopic characteristics before they erach cloud based if dispersed from the surface. Such reactions have direct effects on the dispersal and effectiveness of hygroscopic seeding in polluted environments.

TEM analyses of the ICE 70% flare showed that the larger particles produced by these flares were aggregate mixtures of KCl and $Ca(Cl)_2$ and not single particles. Thus, aggregation or coagulation of particles is an important mechanism for producing larger particles. Chemical analyses identified $Ca(Cl)_2$ as a coating to all aggregates, suggesting this phase acted as a catalyst for aggregation. At this point, we do not fully understand how $Ca(Cl)_2$ acts as a catalyst. It could be related to the micro-scale meteorology around the burning flare, created by very small local regions of high humidity. In these regions, $Ca(Cl)_2$ could deliquesce, and wet other combustion particles, resulting in more efficient coagulation.

Our parcel model calculations for the new ICE 70% flare produced substantially more drizzle drops at shorter times than the original South African flare. Once drizzle formed the transformation to rainwater also proceeded at a faster rate than for the original South African flare. The model results suggest that the ICE 70% is highly suitable for hygroscopic seeding experiments.

Based on our experiments, it appears possible to tailor the particle size distribution of flares to suit specific seeding situations and environments. New flare development technology could explore the use of other materials such as desert dust and organic materials and their specific effects on water and ice nucleation, as well as other microphysical processes in clouds.

References

Bruintjes R.T., D. W. Breed, G.B. Foote, V. Salazar, M. J. Dixon, T. Fowler, and B. G. Brown, 2003: Program for the augmentation of rainfall in Coahuila: Overview and results. *Proc. 8th WMO Scientific Conference On Weather Modification*, April 2003, Casablanca, Morocco, 103-106.

Caro, D, W. Wobrock, and A.I. Flossmann, 2002: A numerical study on the impact of hygroscopic seeding on the development of cloud particle spectra. *J. Appl. Meteor.* Vol?, Pages?.

Cooper, W.A., R.T. Bruintjes, and G.K. Mather, 1997: Some calculations pertaining to hygroscopic seeding with flares. J. Appl. Meteor., **36**, 1449-1469.

Eagen, R.C., P.V. Hobbs, and L.F. Radke, 1974: Particle emissions for a large Kraft paper mill and their effects on the microstructure of warm clouds. *J. Appl. Meteor.*, **13**, 535-552.

Flossmann, A.I., W.D. Hall, and H.R. Pruppacher, 1985: A theoretical study of the wet removal of atmospheric pollutants. Part I. *J. Atmos. Sci.*, **42**, 582-606.

Flossmann A.I., H.R. Prppacher, and J.H. Topalian, 1987: A theoretical study of the wet removal of atmospheric pollutants. Part II. *J. Atmos. Sci.*, **44**, 2912-2923.

Hindman, E.E., II, P.V. Hobbs, and L.F. Radke, 1977: Cloud condensation nuclei from a Paper Mill. Part I: Measured effects on clouds. *J. Appl. Meteor.*, **16**, 745-752.

Hindman, E.E., 1978: Water droplet fogs formed from pyrotechnically generated condensation nuclei. *J. Wea. Modif.*, **10**, 77-96.

Li, J., M. Posfai, P.V. Hobbs, and P.R. Buseck: Individual aerosol particles from biomass burning in southern Africa: 2. Compositions and aging of inorganic particles. J. of Geophys. Res., **108**, D13, 8484, SAF20, 2003.

Mather, G.K., 1991: Coalescence enhancement in large multicell storms caused by the emissions from a kraft paper mill. *J. Climate Appl. Meteor.*, **25**, 1780-1784.

Mather, G.K., D.E. Terblanche, F.E. Steffens, and L. Fletcher, 1997: Results of the South African cloud seeding experiments using hygroscopic flares. *J. Appl. Meteor.*, **36**, 1433-1447.

National Research Council of the National Academy of Sciences, 2003, *Critical Issues in Weather Modification Research*, Board on Atmospheric Sciences and Climate, Division on Earth and Life Studies, National Research Council of the National Academy of Sciences, The National Academy Press, 123pp

Posfai, M., R. Simonics, J. Li, P.V. Hobbs, and P. R. Buseck, Individual aerosol particles from biomass burning in southern Africa: 1. Compositions and size distributions of carbonaceous particles. J. of Geophys. Res., **108**, 8483, SAF20, 2003.

Reisin, T., S. Tzivion, and Z. Levin, 1996: Seeding convective clouds with ice nuclei or hygroscopic particles: A numerical study using a model with detailed microphysics. *J. Appl. Meteor.*, **35**, 1416-1434.

Segal, Y., A. Khain, M. Pinsky nad D. Rosenfeld, 2004: Effects of hygroscopic seeding on raindrop formation as seen from simulations using a 2000-bin spectral cloud parcel model. *Atmos. Research*, **71**, 3-34.

Silverman, B.A. and W. Sukarnjanasat, 2000: Results of the Thailand warm-cloud hygroscopic particle seeding experiment. *J. Appl. Meteor.*, **39**, 1160-1175.

Silverman, B.A., 2003: A critical assessment of hygroscopic seeding of convective clouds for rainfall enhancement. *Bull. Amer. Meteor. Soc.*, **84**, 1219-1230.

Strapp W.J., W.R. Leaitch, P.S.K. Liu, 1992: Hydrated and Dried Aerosol-Size-Distribution Measurements from the Particle Measuring Systems FSSP-300 Probe and the Deiced PCASP-100X Probe. *Journal of Atmospheric and Oceanic Technology*, **9**, No. 5, 548–555.

Terblanche, D.E., F. E. Steffens, L. Fletcher, M. Mittermaier, and R. Parsons, 2000: Towards the operational application of hygroscopic flares for rainfall enhancement in South Africa. *J. Appl. Meteor.*, **39**, 1811-1821.

Tessendorf, S.A., and Co-authors, 2011: The Queensland Cloud Seeding Research Program. *Bull. Amer. Meteor. Soc.*, In press for January 2012 issue.

WMO, 2000: Report of the WMO International workshop on hygroscopic seeding: Experimental results, physical processes, and research needs. WMP Report No. 35, World Meteorological Organization, Geneva Switzerland, 68pp.

Yin, Y., Z. Levin, T. G. Reisin and S. Tzivion, 2000a: Seeding convective clouds with hygroscopic flares; Numerical simulations using a cloud model with detailed microphysics. *J. Apply. Meteor.*, **39**, 1460-1472.

Yin, Y., Z. Levin, T. G. Reisin and S. Tzivion, 2000b: The effects of giant cloud condensation nuclei on the development of precipitation in convective clouds - A numerical study. *Atmos. Res.*, **53**, 91-116.